


Interaction between Cervical Microbiota and Host Gene Regulation in Caesarean Section Scar Diverticulum

Xing Yang,^a Xinyi Pan,^a Manchao Li,^a Zhi Zeng,^a Yanxian Guo,^a Panyu Chen,^a Xiaoyan Liang,^a  Peigen Chen,^a Guihua Liu^a

^aReproductive Medicine Research Center, The Sixth Affiliated Hospital, Sun Yat-sen University, Guangzhou, Guangdong, People's Republic of China



ABSTRACT Cesarean section scar diverticulum (CSD) has become a formidable obstacle preventing women receiving CS from reproducing. However, the pathogenesis of CSD remains unexplored. In this study, we characterized the cervical microbiota, metabolome, and endometrial transcriptome of women with CSD. Based on the 16s rRNA results of cervical microbes, the microbial diversity in the CSD group was higher than that in the control group. *Lactobacillus* were significantly decreased in the CSD group and were mutually exclusive with potentially harmful species (*Sphingomonas*, *Sediminbacterium*, and *Ralstonia*) abnormally elevated in CSD. The microbiota in the CSD group exhibited low activity in carbohydrate metabolism and high activity in fatty acid metabolism, as confirmed by the metabolomic data. The metabolomic characterization identified 6,130 metabolites, of which 34 were significantly different between the two groups. In the CSD group, N-(3-hydroxy-eicosanoid)-homoserine lactone and Ternatin were significantly increased, in addition to the marked decrease in fatty acids due to high consumption. N-(3-hydroxy-eicosanoyl)-homoserine lactone is a regulator that promotes abnormal apoptosis in a variety of cells, including epithelial cells and vascular endothelial cells. This abnormal apoptosis of endometrial epithelial cells and neovascularization was also reflected in the transcriptome of the endometrium surrounding the CSD. In the endometrial transcriptome data, the upregulated genes in the CSD group were active in negatively regulating the proliferation of blood vessel endothelial cells, endothelial cells, and epithelial cells. This alteration in the host's endometrium is most likely influenced by the abnormal microbiota, which appears to be confirmed in the results by integrating host transcriptome and microbiome data. For the first time, this study described the abnormal activity characteristics of microbiota and the mechanism of host-microbiota interaction in CSD.

IMPORTANCE Cesarean section scar diverticulum (CSD) has become a formidable obstacle preventing women receiving CS from reproducing. In this study, we revealed that potentially harmful microbes do have adverse effects on the host endometrium. The mechanism of these adverse effects includes the inhibition of the activity of beneficial bacteria such as lactobacilli, consumption of protective metabolites of the endometrium, and also the production of harmful metabolites. In the present study, we elucidated the mechanism from the perspectives of microbial, metabolic, and host responses, providing an important rationale to design preventive and therapeutic strategies for CSD.

KEYWORDS cesarean section scar diverticulum, gene regulation, host-microbiota interaction, microbiome

Over recent decades, the cesarean section (CS) rate in China rose from 3% in 1988 to 34.9% in 2014, and then to 36.7% in 2018, ranking first among Asian countries (1, 2). Around 19.4% to 88% of women receiving CS will suffer from cesarean section scar diverticulum (CSD) (3). CSD is a result of poor healing of the local uterine incision, forming a depression or cavity that connects with the uterine cavity, which can result in a variety of near- and long-term complications, such as scar dehiscence, ectopic scar pregnancy, uterine rupture, prolonged menstrual bleeding, chronic pelvic pain, and secondary infertility (4, 5).

Editor Florence Claude Doucet-Populaire, University Paris-Saclay, AP-HP Hôpital Antoine Bécélère, Service de Microbiologie, Institute for Integrative Biology of the Cell (I2BC), CEA, CNRS

Ad Hoc Peer Reviewers  Gajender Aleti, University of California, San Diego;  Din Ahmad Ud, West China Hospital of Sichuan University

Copyright © 2022 Yang et al. This is an open-access article distributed under the terms of the [Creative Commons Attribution 4.0 International license](https://creativecommons.org/licenses/by/4.0/).

Address correspondence to Guihua Liu, liuguihua@mail.sysu.edu.cn, Peigen Chen, chenpg@mail2.sysu.edu.cn, or Xiaoyan Liang, liangxy@mail.sysu.edu.cn.

The authors declare no conflict of interest.

Received 8 May 2022

Accepted 1 July 2022

Published 28 July 2022

TABLE 1 The clinical data features of 52 subjects

n	CON 24	CSD 28	P	SMD
Age (mean [SD])	29.62 (3.57)	33.25 (3.17)	<0.001	1.073
BMI (mean [SD])	21.04 (2.25)	22.23 (2.62)	0.088	0.488
AMH (ng/mL; mean [SD])	3.69 (2.09)	3.42 (3.76)	0.761	0.087
Basal_FSH (IU; mean [SD])	6.99 (1.42)	7.62 (1.91)	0.192	0.372
Basal_LH (IU; mean [SD])	5.51 (2.97)	5.59 (3.38)	0.929	0.025
Basal_E2 (pg; mean [SD])	47.42 (68.52)	42.89 (28.19)	0.75	0.086
Infertile_year	3.54 (2.19)	4.64 (2.91)	0.134	0.428

CSD has become a formidable obstacle preventing those women from reproducing. The spontaneous pregnancy rate in CS women has decreased by 15%, and even with assisted reproductive technology, the embryo implantation and live birth rates are significantly lower (6). Our previous research revealed that persistent effusion is the major factor affecting fecundity in CSD women (7).

The female reproductive tract has a unique microbiome that has a critical role in the maintenance of homeostasis and/or development of certain diseases (8–10). When dysbiosis occurs, altered immune and metabolic signaling can produce commensurate responses, including chronic inflammation, epithelial barrier disruption, angiogenesis, and metabolic dysregulation (11–13). Our previous research revealed that persistent effusion in CSD were caused by localized inflammatory and immune imbalance, and local microbial disturbances play a core role in this process (14). However, the characteristics of local microbiota activities and the mechanism of microbial-host interaction are still unknown.

In this study, we combined nontargeted metabolomics and human host transcriptome to analyze the activity characteristics of CSD microbes and the mechanism of microbe-host interaction.

RESULTS

Diversity and compositional characteristics of cervical microbiota. A total of 52 subjects were included in the study, including 28 in the CSD group and 24 in the CON group. The clinical data features of subjects are shown in Table 1. After filtering and quality control, an average of 60833.13 ± 7511.79 reads were obtained from each sample. The rarefaction curve indicated that the sequencing depth of the samples in this study was sufficient (Fig. S1A).

The α -diversity of the microbiota calculated by Shannon-Wiener index at the phylum (Fig. 1A) and genus levels (Fig. 1B) in the CSD group was significantly higher than that in the CON group, indicating that the microbial composition of the CSD group was more abundant. Bray-Curtis-based PCoA plot and ANOSIM analysis showed that the distance between samples in the CSD group was significantly greater than in the CON group (Fig. 1C).

The absolute abundances of phylum (Fig. S1B) and genus (Fig. S1C) in the CSD group were higher than in the CON group. Classification at the phylum level showed a different pattern between the two groups, with *Firmicutes* being the overwhelming majority in the CON group, reaching 92% (Fig. 1D). In the CSD group, the proportion of *Firmicutes* decreased to 62%, and the proportion of *Proteobacteria* and *Actinobacteriota* increased to 20% and 10%, respectively (Fig. 1E). The composition of the two groups at the genus level also showed significant differences.

The present study dissected the genus composition of *Firmicutes* and *Proteobacteria* between the two groups. Under the *Firmicutes* genus, the proportion of *Lactobacillus* in the CSD group (Fig. 1F) decreased compared with that in the CON group (Fig. 1H) (84.91% versus 98.81%), while the proportions of *Streptococcus* and *Enterococcus* increased (7.62% and 3.33%, respectively). The proportions of *Proteobacteria* genera, including *Escherichia*, *Shigella*, *Sphingomonas*, *Ralstonia* and *Burkholderia*, *Caballeronia*, *Paraburkholderia*, showed various degrees of differences between the CSD group (Fig. 1G) and the CON group (Fig. 1I). These results indicated that the diversity and composition of microbiota in the CSD group were

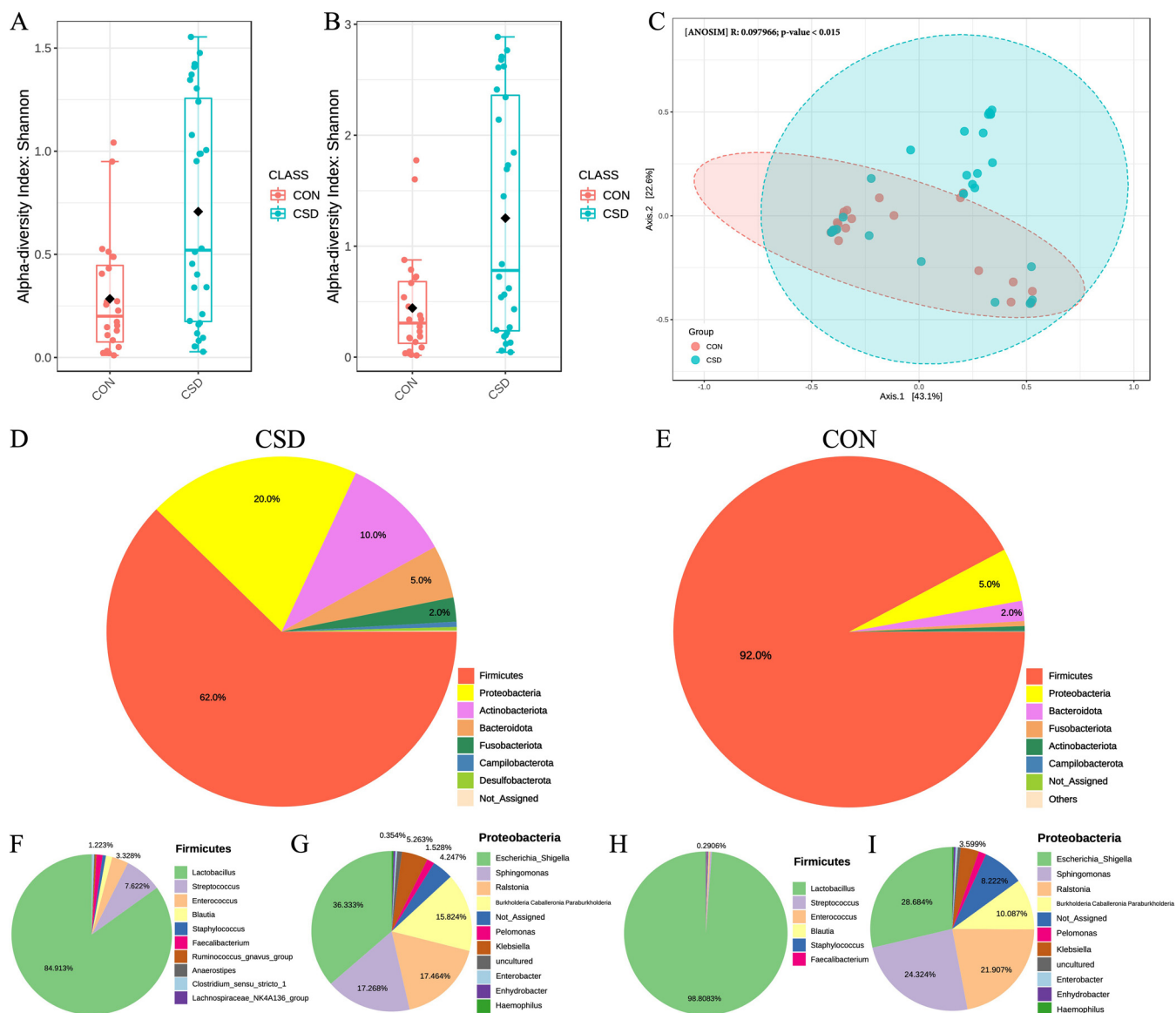


FIG 1 Microbial community characteristics. The α -diversity of the microbiota calculated by Shannon-Wiener index at the phylum (A) and genus levels (B) (Wilcoxon rank sum test); (C) Bray-Curtis-based PCoA plot and Anosim analysis between CSD group and CON group; Pie chart of phylum composition of CSD group (D) and CON group (E); Pie chart of genus composition of *Firmicutes* (F) and *Proteobacteria* (G) in CSD group; Pie chart of genus composition of *Firmicutes* (H) and *Proteobacteria* (I) in CSD group.

significantly different from those in the CON group, and the proportion of *Lactobacilli* significantly decreased in the CSD group.

Screening of differential microbiota and construction of cooccurrence network.

Based on linear discriminant analysis (LDA), differential genus between the two groups were screened. *Lactobacillus* significantly decreased in the CSD group, while *Gardnerella*, *Prevotella*, and other harmful genus increased significantly ($LDA \geq 2$) (Fig. 2A, Table S1).

The genus cooccurrence network (Fig. 2B) constructed based on Spearman correlation analysis ($R > 0.8, P < 0.05$) showed interesting information. The cooccurrence network composed of *Ralstonia*, *Sphingomonas*, and *Sediminbacterium* was significantly negatively correlated with *Lactobacillus*. The abundance of these four genera was opposite between the two groups (Fig. 2C–F). This result suggested that the decrease in *Lactobacillus* abundance might be caused by the disturbance and mutual exclusion of the microbial community.

Functional enrichment analysis of microbiota. The results of PICRUSt 2 characterized the activity of microbiotas in two groups. We analyzed level 2 and level 3 of the KEGG

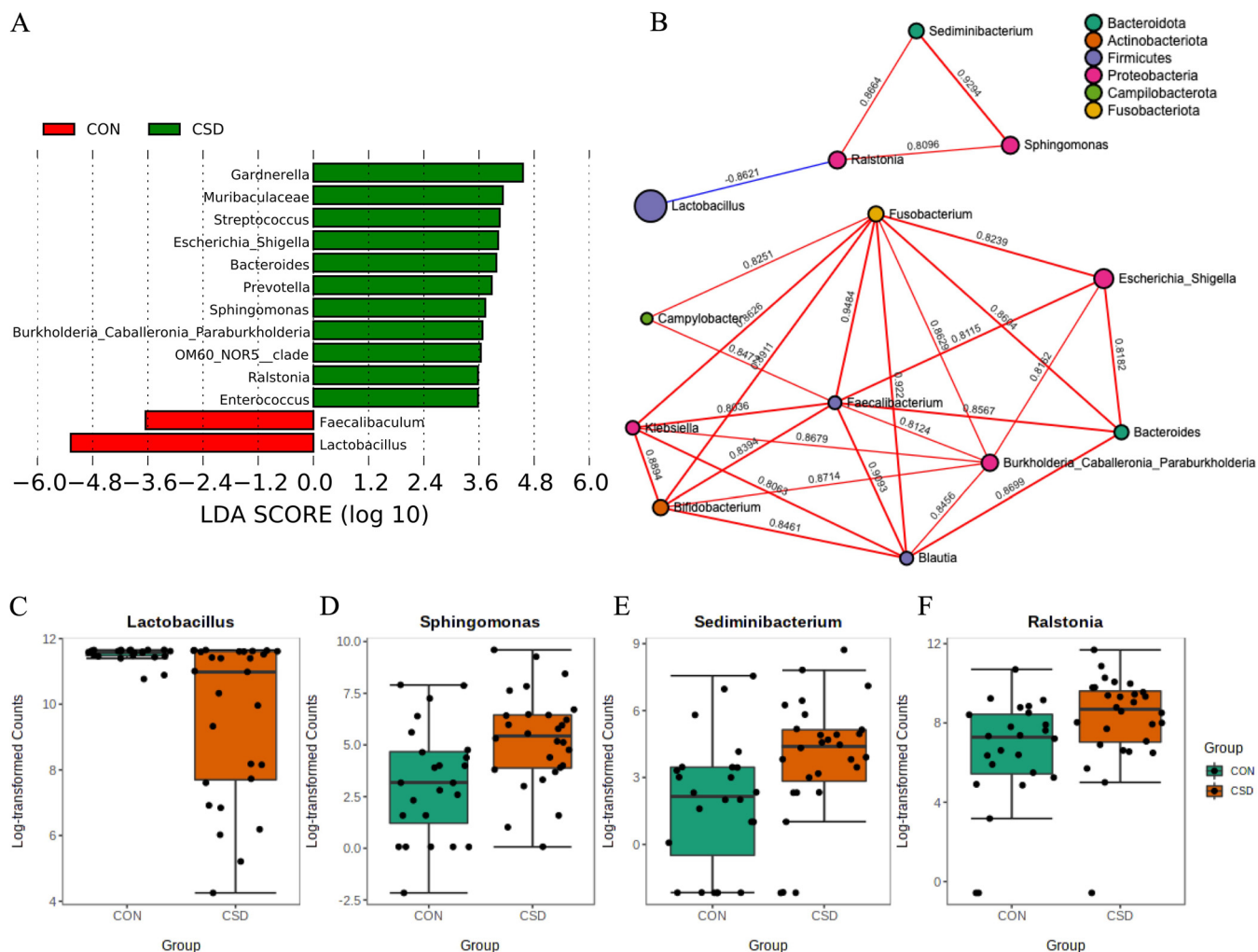


FIG 2 Compositional differences and cooccurrence relationships of microbiota. (A) Differential genera between CSD group and CON group; (B) Cooccurrence networks of microbial communities (Spearman correlation analysis). The data on the line is the correlation coefficient. The size of the dots indicates the abundance of the genus; The abundance of *Lactobacillus* (C), *Sphingomonas* (D), *Sediminibacterium* (E), and *Ralstonia* (F) in CSD group and CON group (Wilcoxon rank sum test).

pathway, respectively. The CSD group showed significant activity in multiple metabolic processes, except for carbohydrate metabolism, an important pathway for lactate production (Fig. 3A). In a more refined pathway (level 3, Fig. 3B), the CSD group showed high activity in the fatty acid metabolism pathway and the biosynthesis of secondary metabolites, whereas the active carbohydrate metabolism pathway in the CON group was refined to glucose metabolism. Phosphotransferase system (PTS) and Fructose & mannose metabolism in the CON group were also more active than in the CSD group (Fig. 3B). The *P*-values were corrected using the BH (Benjamini and Hochberg) method.

Nontargeted metabolomics in the cervical environment. We performed simultaneous nontargeted metabolomic assays on samples from 60 subjects. After quality control (Fig. S2), 46 microbiome-matched samples were included in the subsequent analysis, including 20 samples from the CON group and 26 samples from the CSD group. After noise removal, 10,119 anion peaks and 8,308 cation peaks were obtained. The ion peaks with all missing values in the group (0 value) > 50% were deleted, and we replaced the 0 value with half of the minimum value and deleted the qualitative result score less than 36 points. As a result, we obtained 6,130 metabolites.

OPLS-DA was used to discriminate overall differences in metabolic profiles and further identify differential metabolites between groups. The results indicated that the samples

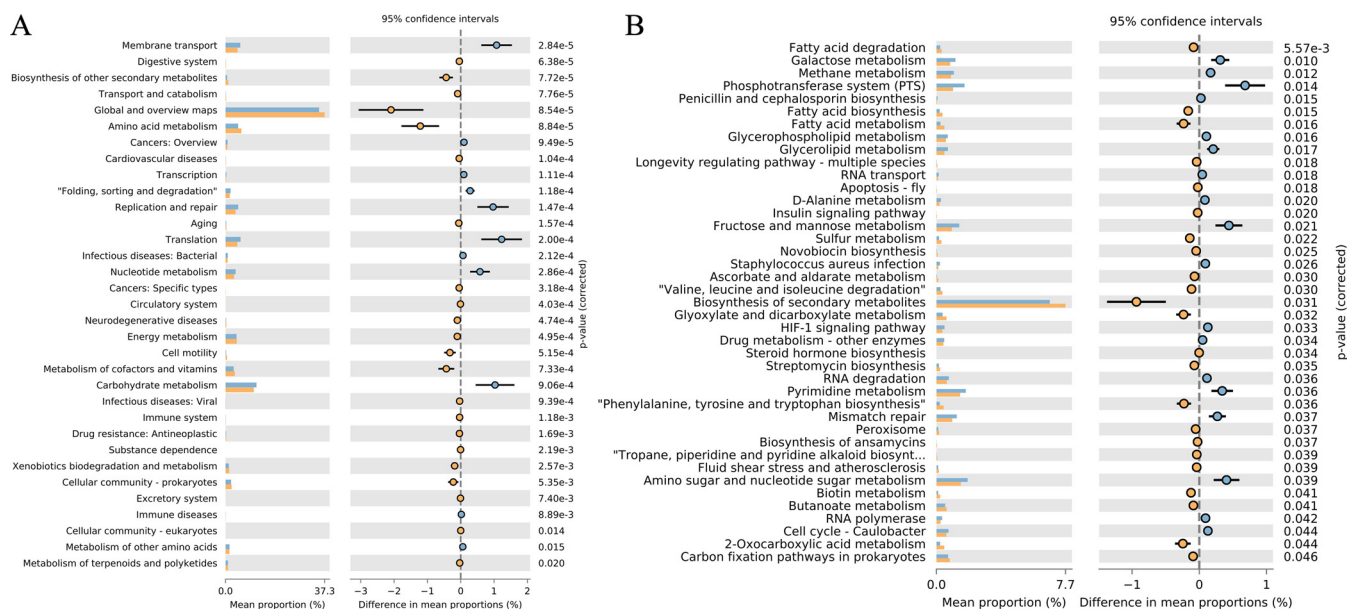


FIG 3 Functional characterization of cervical microbes. Difference between CSD group and CON group in KEGG level 2 (A) and level 3 (B) (Welch's *t* test).

within the CSD group were clustered together and differed from the overall profile of the CON group (Fig. 4A, B). Thirty-four metabolites that differed significantly between the two groups were identified (Fig. 4C, Table S2). Two metabolites were significantly upregulated in the CSD group; namely, N-(3-hydroxy-eicosanoyl)-homoserine lactone and Ternatin. 32 metabolites were significantly downregulated, and the two most significantly downregulated metabolites were Gingerol and PC(O-10:0/O-8:0)[U].

Correlation between cervical microbiota and metabolome. To further explore the pathogenic mechanisms of cervical microbes in CSD, we performed an integrative analysis of the cervical microbiome and metabolome (Fig. 5). The results showed a trend consistent with the cooccurrence network (Fig. 2B). We found that many metabolites that were positively correlated with *Lactobacillus* were negatively correlated with *Prevotella*, *Sphingomonas*, *Ralstonia*, etc. Two metabolites were significantly positively associated with *Lactobacillus*, including Antanapeptin C ($R = 0.39$) and 3-Epipapyriteric acid ($R = 0.39$). However, N-Acetyl-a-neuraminic acid, N-Acetyl-b-neuraminic acid, N-(3-hydroxy-eicosanoyl)-homoserine lactone, and Ternatin were negatively correlated with various genus mutually exclusive with *Lactobacillus*.

Human host endometrial response. To further understand the human host response to a disturbed microbial community, we performed transcriptome sequencing of endometrium surrounding the cesarean section scar diverticulum. We performed transcriptome analysis of 33 samples paired with the microbiome and metabolome, including 18 samples from the CSD group and 15 samples from the CON group. A total of 982 differentially expressed genes were identified between the two groups (Fig. 6A), including 176 genes that were upregulated in CSD, and 806 that were downregulated (Fig. 6B, Table S3). We noted that upregulated genes in the CSD group negatively regulated the proliferation of blood vessel endothelial cells, endothelial cells, and epithelial cells (Fig. 6C). At the same time, these genes were also active in the endothelial cell apoptotic process. This suggest that local angiogenesis was hindered in the CSD group. Downregulated genes were mainly concentrated in immune system-related processes (Fig. 6D).

The integration of microbes and transcriptomes was achieved by constructing the O2PLS model. After 10-fold cross-validation, the model building parameters were finally set as $n = 5$, $n_x = 3$, $n_y = 1$, and the R2X was 0.91 and R2Y was 0.90 (Fig. 7A). These two parameters indicate that the model is reliable. Fig. 7B shows the top 15 loading features of the two omics.

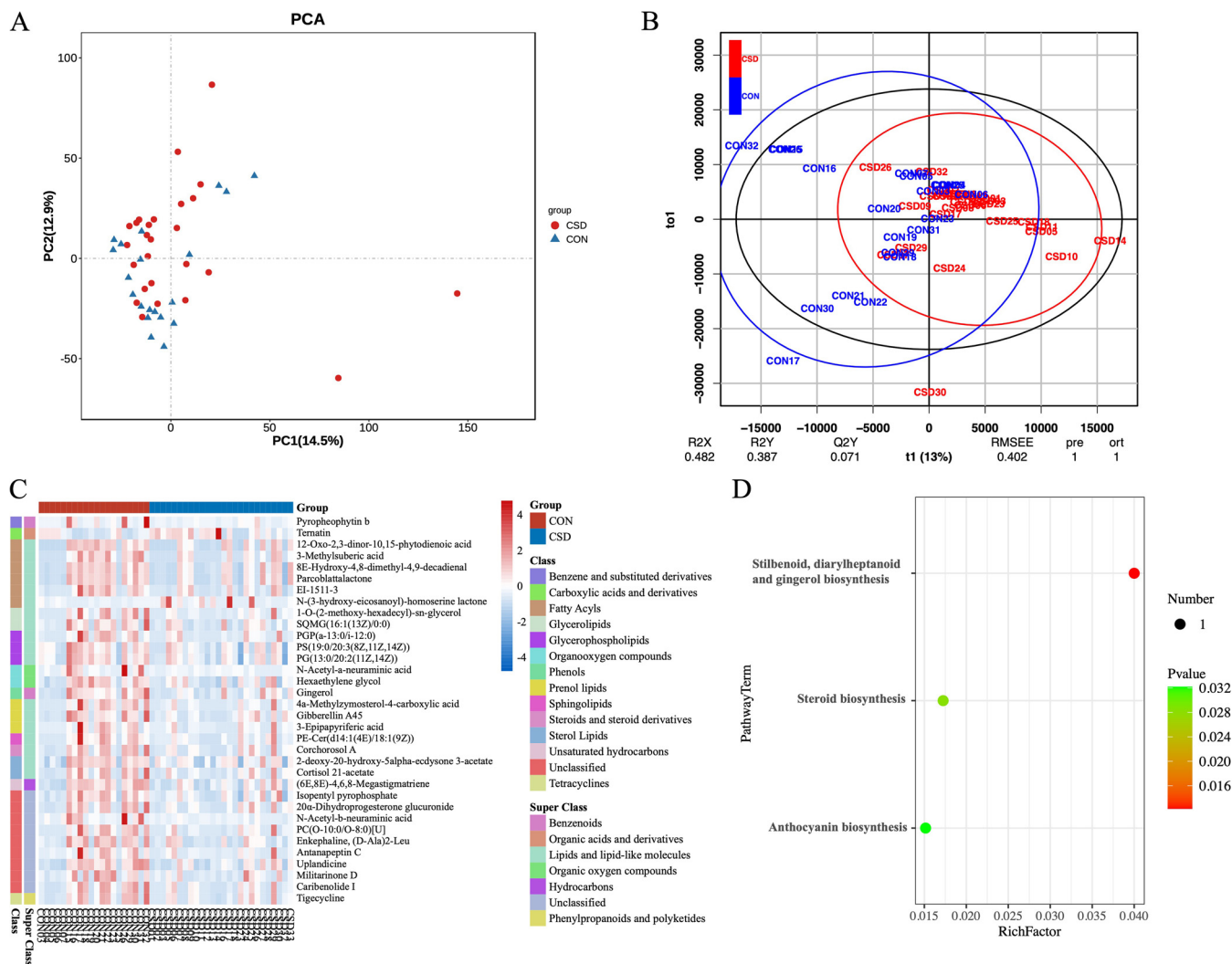


FIG 4 Nontargeted metabolomics in the cervical environment. (A) PCA plots of the two groups of metabolites; (B) OPLS-DA score map. The abscissa represents the score value of the principal component, and the ordinate represents the score value of the orthogonal component; (C) Heatmap of differential metabolites between two groups; (D) KEGG enrichment analysis of differential metabolites.

We performed Spearman correlation analysis on the characteristics of top 30 loading in the two groups, trying to find out the relationship between specific genus and genes. We found several specific genes, including DKK1, CXCL14, SCARA5, APOD, S100A4, CFD, GPX3, and HBB. These genes were significantly positively correlated with genus mutually exclusive with *Lactobacillus* (Fig. 2B) but negatively correlated with *Lactobacillus* (Fig. 7C). The results of functional enrichment analysis of these genes showed that they were mainly active in the negative regulation of cell junction assembly and the process of epithelial to mesenchymal transition (Fig. 7D). Cell junction assembly was an essential process of angiogenesis. This result indicated that angiogenesis disorders and intimal hyperplasia disorders during the formation of CSD were closely related to microbial disorders.

DISCUSSION

Cesarean section scar diverticulum (CSD) is a huge obstacle for those women who wish to have more children. This study attempted to explain the impact of cervical microbiota and metabolites on women with CSD from multiple perspectives, including the microbial perspective and the human host response perspective.

This study observed that the structure of cervical microbiota in the CSD group was different from that in the control group. *Lactobacillus* significantly decreased in CSD group,

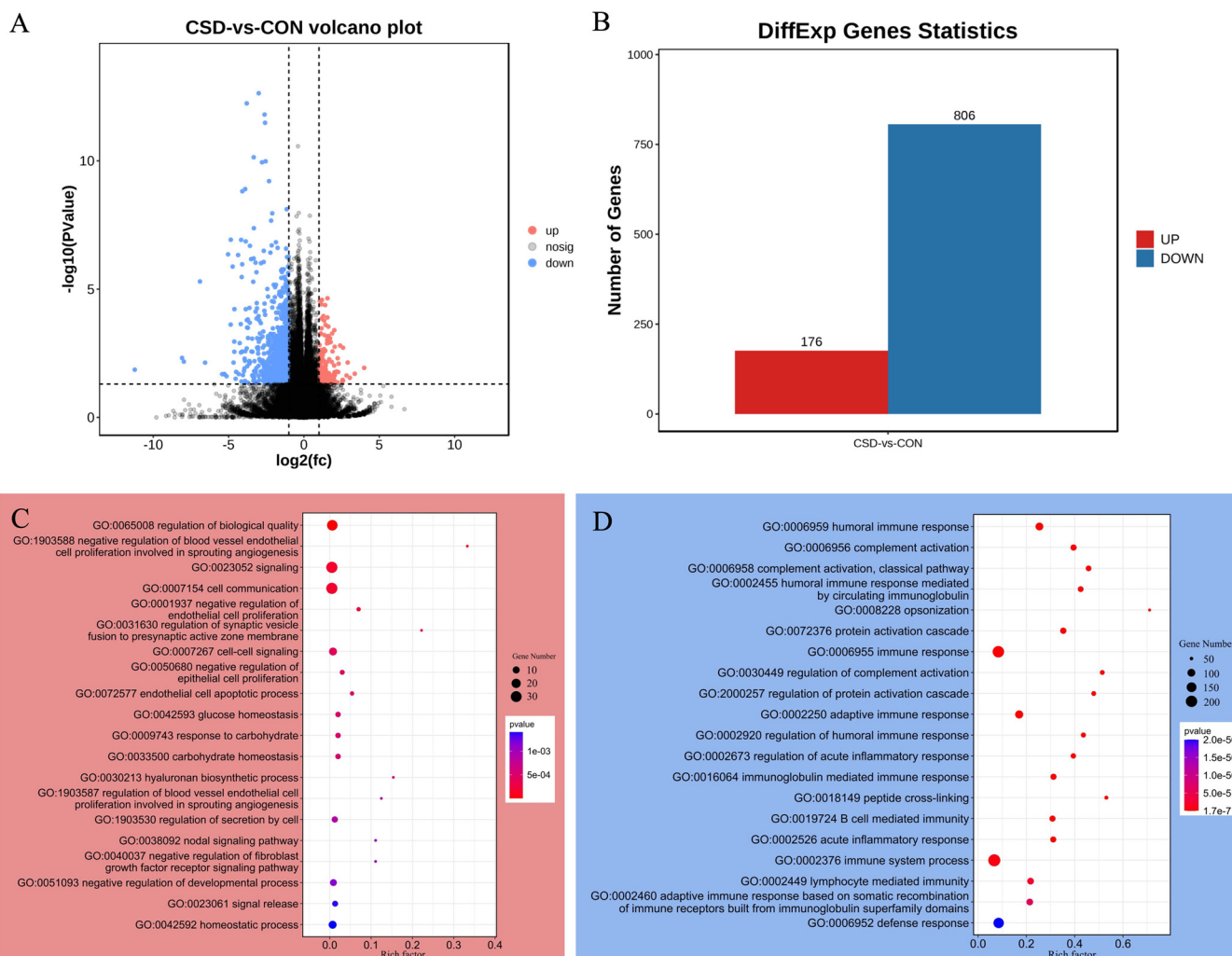


FIG 6 Endometrial transcriptome expression characteristics. (A) Volcano plot for differential gene expression analysis; (B) Statistical chart of differentially expressed genes between CSD group and CON group; GO enrichment analysis of biological processes of upregulated (C) and downregulated (D) genes.

have protective effects on the endometrium, including 12-Oxo-2,3-dinor-10,15-phytodienoic acid, and 3-Methylsuberic acid (22). N-(3-hydroxy-eicosanoyl)-homoserine lactone has been shown to promote apoptosis of various cells *in vivo*, including macrophages (23), vascular endothelial cells (24), and fibroblasts (25), through mitochondrial damage received by reactive oxygen species. Interestingly, 12-Oxo-2,3-dinor-10,15-phytodienoic acid and N-(3-hydroxy-eicosanoyl)-homoserine lactone had the opposite relationship with the potentially harmful genus and *Lactobacillus*. The metabolomic results reconfirmed the mutually exclusive relationships in the cooccurrence network we found based on the microbiome data, namely, that the abundance and activity of *Lactobacillus* were significantly suppressed, and multiple beneficial fatty acids were largely consumed.

Although we had thoroughly explored the mechanisms and possible effects of microbial community disturbance in the CSD group, such as the discovery of potential pathogenic bacteria through the inhibition of *Lactobacillus* and the production of deleterious metabolism such as N-(3-hydroxy-eicosanoyl)-homoserine lactone, it is still unclear whether the human host was affected by these effects. Therefore, we performed transcriptome sequencing of the endometrium surrounding the CSD.

Surprisingly, we found changes in the transcriptome in the endometrium corresponding

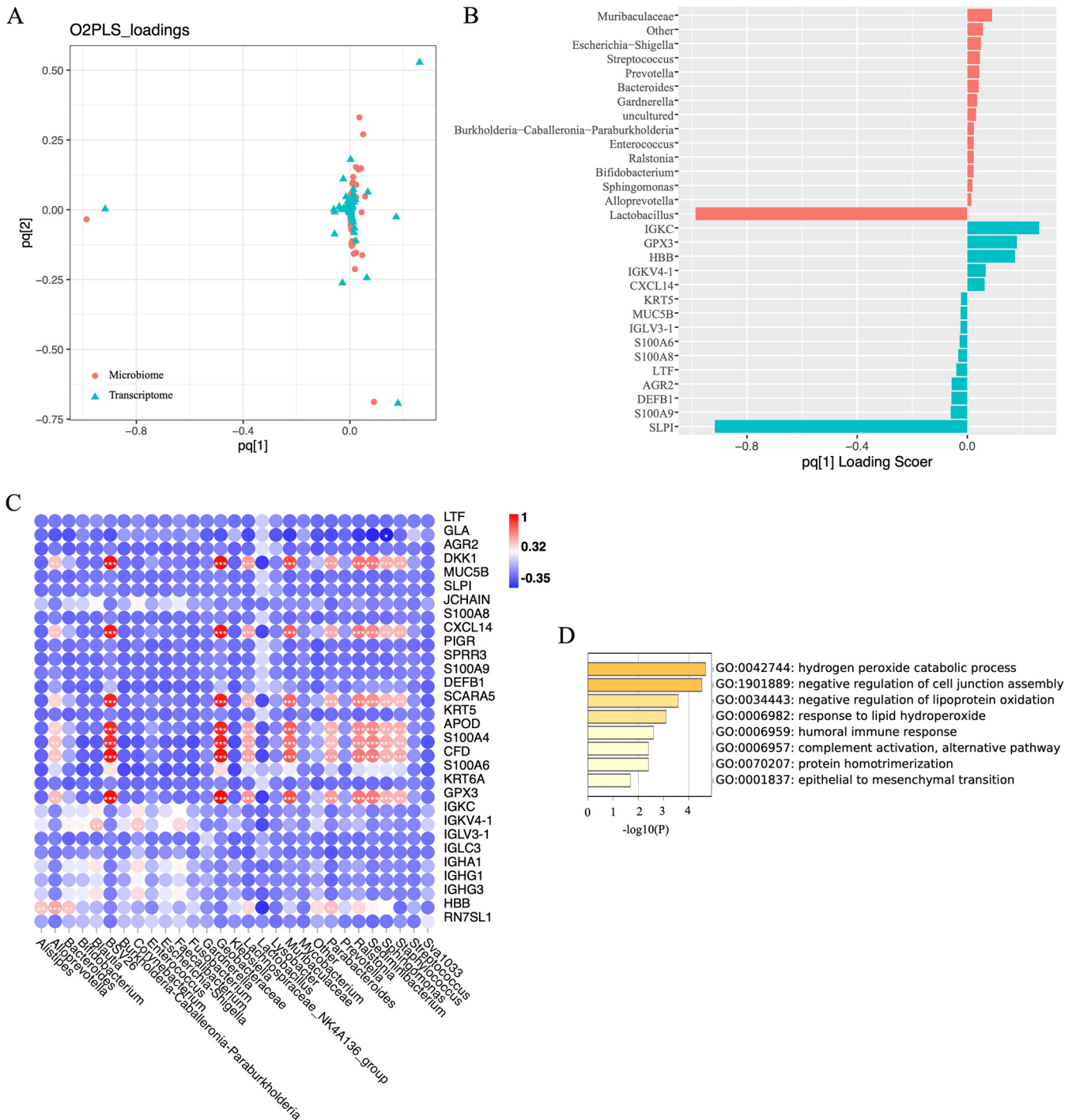


FIG 7 Host-microbiota interaction analysis. (A) Loading scatterplot of the O2PLS model. The farther from the origin, the correlation of features is about stronger; (B) Bar graph of top 15 loading features in the microbiome and transcriptome. The characteristic trends in the same direction are consistent; (C) Heatmap of correlation analysis of top 30 loading features in both groups; (D) Functional enrichment analysis of Sphingomonas, Sediminbacterium, and Ralstonia-related genes.

to the above findings. GO enrichment analysis of the significantly upregulated genes in the CSD group showed that these genes were concentrated in the biological processes of negatively regulating the proliferation of blood vessel endothelial cells, endothelial cells, and epithelial cells. After integrating the microbiome and transcriptome data, we found that the genes regulating these functions were potentially pathogenic bacteria identified in the

previous data, including *Ralstonia*, *Sphingomonas*, and *Sediminbacterium*. *Lactobacillus* was negatively correlated with these adverse biological activities.

So far, we had revealed that potentially harmful microbes do have adverse effects on the host endometrium. The mechanism of these adverse effects includes the inhibition of the activity of beneficial bacteria such as *Lactobacilli*, consumption of protective metabolites of the endometrium, and also the production of harmful metabolites. However, the 16s rRNA sequencing method applied in this study has its limitations, such as short read lengths obtained and low species resolution (26, 27). In addition, the host's response requires more dimensions of experiments to aid validation. To our knowledge, this is the first study to detail the pathogenic mechanism of microbial community disturbance in CSD. Using the composition and activity characteristics of microbiota, ideas have been developed for the development of new and more effective probiotic formulations. At present, it has been reported that the *Lactobacillus rhamnosus* BPL005 strain can improve the health of the female reproductive tract (28). In addition, another study showed that among non-*Lactobacillus*-dominant patients treated with lactoferrin for 3 months after antibiotic treatment, 67% (6/9) of the patients had a return of the endometrial microbiota to a *Lactobacillus*-dominant environment (12, 29). These studies suggest that a combination of probiotics combined with prebiotics, such as lactoferrin, may have potential therapeutic benefits. An interventional study of *Lactobacillus* preparations is also under way, and we will announce the results of the study shortly. In the present study, we elucidated the mechanism from the perspectives of microbial, metabolic, and host responses, providing an important rationale to design preventive and therapeutic strategies for CSD.

Conclusion. Cervical microbiota in women with CSD had higher microbial diversity and lower *Lactobacillus* abundance. The cooccurrence network composed of *Ralstonia*, *Sphingomonas* and *Sediminbacterium* was mutually exclusive with *Lactobacillus* and inhibited local neovascularization and promoted apoptosis of vascular endothelial cells and endometrial epithelial cells by depleting protective fatty acids and producing N-(3-hydroxy-eicosanoyl)-homoserine lactone.

MATERIALS AND METHODS

Collection of research subjects and ethical approval. Parous women underwent hysteroscopy at the Sixth Affiliated Hospital of Sun Yat-sen University in 2021 were enrolled in this case-control study. The inclusion criteria were (i) 20 to 40 years old; (ii) secondary infertility; (iii) normal karyotype; (iv) informed consent. The exclusion criteria included (i) acute pelvic inflammation, cervicitis, or vaginitis; (ii) endometriosis or adenomyosis; (iii) history of tuberculosis infection; (iv) antibiotics, glucocorticoids, or immunosuppressants received within a month before hysteroscopy; (v) sexual activity, vaginal irrigation, or drug application within 48 h before sampling. Parous women with post-cesarean section scar diverticulum (4, 5) were separated into the CSD group, and those who had vaginal deliveries were separated into the control group (CON group).

All study procedures were reviewed and approved by the ethics review board of the Sixth Affiliated Hospital of Sun Yat-Sen University (IRB no. 2019ZSLYEC-0055).

Sample collection procession. Cervix specimens were collected by using a sterile single-tipped CultureSwab. The swab was inserted into the cervix before hysteroscopy, rotated 360°, held for 10 s, removed and placed into the sterile collection tube, then stored at -80°C , avoiding vaginal walls contact. Uterine endometrium was taken from lower segment during hysteroscopy and immersed in 1 mL of RNAsafer reagent (R4811-02, Magen, China). Endometrial specimens were stored at 4°C overnight before transfer to -80°C .

16S rRNA extraction and sequencing. The universal primers 341F (5'-CTACGGGNGGCWGCAG-3') and 805R (5'-GACTACHVGGGTATCTAATCC-3') were used for 16s rRNA genes sequencing (30). DNA extraction and library construction were as described in our previous study (7). In short, according to the manufacturer's instructions, we used Magpure Soil DNA LQ kit (MAGEN, D6356-02) to conduct a total DNA extraction. PCR amplification was performed by Tks Gflex DNA polymerase (TaKaRa, R060B). After purification and quality control, NovaSeq 6000 (PE250) was used for high-throughput sequencing.

Cervical microbiota analysis. Raw data in the FASTQ format after Cutadapt software (31) was analyzed by QIIME2 (32). According to the default parameters of QIIME2, DADA2 (33) was used to perform quality filtering, noise reduction, splicing, and defitting and, finally, to obtain representative sequences and ASV abundance forms. Based on the Silva (Version138) (34) database, we used a q2-feature-classifier (35) to make a species comparison annotation. Features (ASVs) that count less than 1 in 10% of the sample were excluded.

The microbial diversity of cervical samples was estimated using Alpha diversity metrics inferred by the Shannon index (36). At the same time, the Wilcoxon rank-sum test was used to compare the diversity of the two groups. The Bray Curtis distance matrix was used in Bray Curtis principal

coordinates analysis (PCOA). Analysis of group Similarities (ANOSIM) was used to calculate statistical significance.

LefSe (linear discriminant analysis effect size) (37) was used for differential analysis of cervical microbiota abundance.

We used Spearman correlation analysis to construct the correlation network between genus in Microbiome Analyst with $R > 0.8$ and $P < 0.05$ as cutoff values (38, 39).

PICRUSt2 (phylogenetic investigation of communities by reconstruction of unobserved states) (40) was used for predictive analysis of microbial function. Functional differences between groups were calculated by STAMP V2.1.3 (statistical analysis of taxonomic and functional profiles) (41).

Nontargeted metabolomics. We extracted metabolites from cervical swabs by adding 20 μL of separation buffer (methanol/acetonitrile/water [2:2:1]) to 1 mg of cervical secretions. A 10 μL isolate mix from all samples was set up as a quality control (QC) sample and used to assess stability during the experiment (42). 2 μL of isolate per sample was used to detect the signal of metabolites in all samples by liquid chromatography (LC) and mass spectrometry (MS) (ACQUITY UPLC I-Class plus, Waters). Raw data were qualitatively analyzed by metabolomics processing software Progenesis Q1 v2.3 with parameters of 5 ppm precursor tolerance, 10 ppm product tolerance, and 5% product ion threshold (Nonlinear Dynamics, Newcastle, UK). The internal standard normalization method was used for normalization of all output data, and the results were expressed as peak values (test sample peak area/internal standard sample peak area). Based on accurate mass-to-charge ratio (M/z), secondary fragmentation, and isotopic distributions, we used the Human Metabolome Database (HMDB), Lipidmaps (V2.3), Metlin, EMDB, PMDB, and self-built databases for compound identification.

The differential metabolites between the two groups were selected by the OPLS-DA (orthogonal partial least-squares discriminant analysis) method with VIP value of the first principal component > 1 , and the P -value value of the T -test < 0.05 as cutoff. MetPA was used for differential metabolic pathway analysis (43).

In addition, Spearman correlation analysis was used to assess the correlation of microbiota with metabolites.

Host RNA extraction and sequencing. RNA extraction was performed using the RNeasy minikit (number 74104; Qiagen). Sequencing libraries were then generated using the NEBNext Ultra RNA Library Prep kit according to the manufacturer's instructions. Library preparations were sequenced on the NovaSeq 6000 (Illumina, Inc.) to generate 150 bp paired-end reads.

Host RNA-seq analysis. Trim Galore software was used for raw data quality control and junction trimming. We aligned the filtered raw data to the GRCh38 human genome using HISAT2 (44) software. The feature counts function (45) of the subread software (46) was used for gene quantification. The obtained count gene expression matrix was normalized to TPM (transcripts per kilobase of exon model per million mapped reads). The differentially expressed genes (DEGs) between the CSD group and CON group were selected by DESeq2 R package (P value < 0.05 and log fold change > 1) (47). Clusterprofiler R package (48) was used for functional enrichment analysis of DEGs.

Host-microbiota interaction analysis. In order to clarify the response mechanism of the human host's endometrium to microbial disturbances, the two-way orthogonal PLS (O2PLS) model was constructed for the integrated analysis of DEGs and genus using OmicsPLS R package (49). Spearman correlation analysis was used to determine the relationship between top30 loading DEGs and genus.

Data availability. The 16s rRNA gene sequencing have been deposited with China National Center for Bioinformatics (<https://ngdc.cncb.ac.cn/>) under reference number [PRJCA009374](https://ngdc.cncb.ac.cn/record/PRJCA009374). The transcriptome sequencing for endometrium samples have been deposited with China National Center for Bioinformatics under reference number [PRJCA009373](https://ngdc.cncb.ac.cn/record/PRJCA009373). Raw metabolome data are placed in Metabolights (<http://www.ebi.ac.uk/metabolights/>) under reference number [MTBLS4967](https://www.ebi.ac.uk/metabolights/record/MTBLS4967).

SUPPLEMENTAL MATERIAL

Supplemental material is available online only.

SUPPLEMENTAL FILE 1, PDF file, 1.2 MB.

SUPPLEMENTAL FILE 2, XLSX file, 0.01 MB.

SUPPLEMENTAL FILE 3, XLSX file, 0.01 MB.

SUPPLEMENTAL FILE 4, XLSX file, 0.1 MB.

ACKNOWLEDGMENTS

We thank the Shanghai Luming Biological Technology Co., Ltd. (Shanghai, China) for providing metabolomics services.

We declare that we have no conflicts of interest to disclose.

This study was supported by "Excellent Talents Training Project" of The Sixth Affiliated Hospital of Sun Yat-sen University (grant number R20210217202601970).

G.L., P.C., and X.Y. carried out the study. P.C. and X.Y. analyzed and interpreted the data and drafted the manuscript. X.P., M.L., Z.Z., and X.L. collected the samples. Y.G. and P.C. followed up and collected the clinical data. G.L., P.C., and X.Y. coordinated the study,

participated in the design, and reviewed the manuscript. All authors read and approved the final manuscript.

REFERENCES

1. Qiao J, Wang Y, Li X, Jiang F, Zhang Y, Ma J, Song Y, Ma J, Fu W, Pang R, Zhu Z, Zhang J, Qian X, Wang L, Wu J, Chang H-M, Leung PCK, Mao M, Ma D, Guo Y, Qiu J, Liu L, Wang H, Norman RJ, Lawn J, Black RE, Ronsmans C, Patton G, Zhu J, Song L, Hesketh T. 2021. A Lancet Commission on 70 years of women's reproductive, maternal, newborn, child, and adolescent health in China. *Lancet* 397:2497–2536. [https://doi.org/10.1016/S0140-6736\(20\)32708-2](https://doi.org/10.1016/S0140-6736(20)32708-2).
2. Li HT, Hellerstein S, Zhou YB, Liu JM, Blustein J. 2020. Trends in Cesarean delivery rates in China, 2008–2018. *JAMA* 323:89–91. <https://doi.org/10.1001/jama.2019.17595>.
3. Tower AM, Frishman GN. 2013. Cesarean scar defects: an underrecognized cause of abnormal uterine bleeding and other gynecologic complications. *J Minim Invasive Gynecol* 20:562–572. <https://doi.org/10.1016/j.jmig.2013.03.008>.
4. Schepker N, Garcia-Rocha GJ, von Versen-Hoynck F, Hillemanns P, Schippert C. 2015. Clinical diagnosis and therapy of uterine scar defects after caesarean section in non-pregnant women. *Arch Gynecol Obstet* 291:1417–1423. <https://doi.org/10.1007/s00404-014-3582-0>.
5. Gubbini G, Centini G, Nascetti D, Marra E, Moncini I, Bruni L, Petraglia F, Florio P. 2011. Surgical hysteroscopic treatment of cesarean-induced isthmocele in restoring fertility: prospective study. *J Minim Invasive Gynecol* 18:234–237. <https://doi.org/10.1016/j.jmig.2010.10.011>.
6. Vissers J, Hehenkamp W, Lambalk CB, Huirne JA. 2020. Post-Caesarean section niche-related impaired fertility: hypothetical mechanisms. *Hum Reprod* 35:1484–1494. <https://doi.org/10.1093/humrep/deaa094>.
7. Cai M, Pan X, Xia W, Liang X, Yang X. 2022. Intra-cavitary fluid resulted from caesarean section but not isthmocele compromised clinical pregnancy after IVF/ICSI treatment. *Arch Gynecol Obstet* <https://doi.org/10.1007/s00404-022-06436-0>.
8. Evans J, Salamonsen LA, Winship A, Menkhorst E, Nie G, Gargett CE, Dimitriadis E. 2016. Fertile ground: human endometrial programming and lessons in health and disease. *Nat Rev Endocrinol* 12:654–667. <https://doi.org/10.1038/nrendo.2016.116>.
9. Benner M, Ferwerda G, Joosten I, van der Molen RG. 2018. How uterine microbiota might be responsible for a receptive, fertile endometrium. *Hum Reprod Update* 24:393–415. <https://doi.org/10.1093/humupd/dmy012>.
10. Koedooder R, Mackens S, Budding A, Fares D, Blockeel C, Laven J, Schoenmakers S. 2019. Identification and evaluation of the microbiome in the female and male reproductive tracts. *Hum Reprod Update* 25:298–325. <https://doi.org/10.1093/humupd/dmy048>.
11. Moreno I, Codoñer FM, Vilella F, Valbuena D, Martínez-Blanch JF, Jimenez-Almazán J, Alonso R, Alamá P, Remohí J, Pellicer A, Ramon D, Simon C. 2016. Evidence that the endometrial microbiota has an effect on implantation success or failure. *Am J Obstet Gynecol* 215:684–703. <https://doi.org/10.1016/j.ajog.2016.09.075>.
12. Molina N, Sola-Leyva A, Saez-Lara M, Plaza-Diaz J, Tubić-Pavlović A, Romero B, Clavero A, Mozas-Moreno J, Fontes J, Altmäe S. 2020. New opportunities for endometrial health by modifying uterine microbial composition: present or future? *Biomolecules* 10:593. <https://doi.org/10.3390/biom10040593>.
13. Chen P, Chen P, Guo Y, Fang C, Li T. 2021. Interaction between chronic endometritis caused endometrial microbiota disorder and endometrial immune environment change in recurrent implantation failure. *Front Immunol* 12:748447. <https://doi.org/10.3389/fimmu.2021.748447>.
14. Yang X, Pan X, Cai M, Zhang B, Liang X, Liu G. 2021. Microbial flora changes in Cesarean section uterus and its possible correlation with inflammation. *Front Med (Lausanne)* 8:651938. <https://doi.org/10.3389/fmed.2021.651938>.
15. Martin DH, Marrazzo JM. 2016. The vaginal microbiome: current understanding and future directions. *J Infect Dis* 214 Suppl 1:S36–S41. <https://doi.org/10.1093/infdis/jiw184>.
16. Delgado-Diaz DJ, Tyssen D, Hayward JA, Gugasyan R, Hearn AC, Tachedjian G. 2019. Distinct immune responses elicited from cervicovaginal epithelial cells by lactic acid and short chain fatty acids associated with optimal and non-optimal vaginal microbiota. *Front Cell Infect Microbiol* 9:446.
17. Fang RL, Chen LX, Shu WS, Yao SZ, Wang SW, Chen YQ. 2016. Barcoded sequencing reveals diverse intrauterine microbiomes in patients suffering with endometrial polyps. *Am J Transl Res* 8:1581–1592.
18. Qingqing B, Jie Z, Songben Q, Juan C, Lei Z, Mu X. 2021. Cervicovaginal microbiota dysbiosis correlates with HPV persistent infection. *Microb Pathog* 152:104617. <https://doi.org/10.1016/j.micpath.2020.104617>.
19. de Vos WM, Vaughan EE. 1994. Genetics of lactose utilization in lactic acid bacteria. *FEMS Microbiol Rev* 15:217–237. <https://doi.org/10.1111/j.1574-6976.1994.tb00136.x>.
20. Maia J, Fonseca BM, Teixeira N, Correia-da-Silva G. 2020. The fundamental role of the endocannabinoid system in endometrium and placenta: implications in pathophysiological aspects of uterine and pregnancy disorders. *Hum Reprod Update* 26:586–602. <https://doi.org/10.1093/humupd/dmaa005>.
21. Hamza MS, Ramadan E, Salama SA. 2021. Glucose and fatty acid metabolism involved in the protective effect of metformin against ulipristal-induced endometrial changes in rats. *Sci Rep* 11:8863. <https://doi.org/10.1038/s41598-021-88346-w>.
22. Chen M, Zheng Z, Shi J, Shao J. 2021. Insight on polyunsaturated fatty acids in endometrial receptivity. *Biomolecules* 12:36. <https://doi.org/10.3390/biom12010036>.
23. Woo K, Kim DH, Oh MH, Park HS, Choi CH. 2021. N-3-hydroxy dodecanoyl-DL-homoserine lactone (OH-dDHL) triggers apoptosis of bone marrow-derived macrophages through the ER- and mitochondria-mediated pathways. *Int J Mol Sci* 22.
24. Shin J, Ahn SH, Kim SH, Oh DJ. 2021. N-3-oxododecanoyl homoserine lactone exacerbates endothelial cell death by inducing receptor-interacting protein kinase 1-dependent apoptosis. *Am J Physiol Cell Physiol* 321: C644–C53. <https://doi.org/10.1152/ajpcell.00094.2021>.
25. Neely AM, Zhao G, Schwarzer C, Stivers NS, Whitt AG, Meng S, et al. 2018. N-(3-Oxo-acyl)-homoserine lactone induces apoptosis primarily through a mitochondrial pathway in fibroblasts. *Cell Microbiol* 20:e12787. <https://doi.org/10.1111/cmi.12787>.
26. Quince C, Lanzén A, Curtis TP, Davenport RJ, Hall N, Head IM, Read LF, Sloan WT. 2009. Accurate determination of microbial diversity from 454 pyrosequencing data. *Nat Methods* 6:639–641. <https://doi.org/10.1038/nmeth.1361>.
27. Quince C, Lanzén A, Davenport RJ, Turnbaugh PJ. 2011. Removing noise from pyrosequenced amplicons. *BMC Bioinformatics* 12:38. <https://doi.org/10.1186/1471-2105-12-38>.
28. Chenoll E, Moreno I, Sánchez M, Garcia-Grau I, Silva Á, González-Monfort M, Genovés S, Vilella F, Seco-Durban C, Simón C, Ramón D. 2019. Selection of new probiotics for endometrial health. *Front Cell Infect Microbiol* 9:114. <https://doi.org/10.3389/fcimb.2019.00114>.
29. Kyono K, Hashimoto T, Kikuchi S, Nagai Y, Sakuraba Y. 2019. A pilot study and case reports on endometrial microbiota and pregnancy outcome: an analysis using 16S rRNA gene sequencing among IVF patients, and trial therapeutic intervention for dysbiotic endometrium. *Reprod Med Biol* 18: 72–82. <https://doi.org/10.1002/rmb2.12250>.
30. Hugerth LW, Wefer HA, Lundin S, Jakobsson HE, Lindberg M, Rodin S, Engstrand L, Andersson AF. 2014. DegePrime, a program for degenerate primer design for broad-taxonomic-range PCR in microbial ecology studies. *Appl Environ Microbiol* 80:5116–5123. <https://doi.org/10.1128/AEM.01403-14>.
31. Martin M. Cutadapt removes adapter sequences from high-throughput sequencing reads. 2011. *EMBnet* 17(1):10–12. <https://doi.org/10.14806/ej.17.1.200>.
32. Bolyen E, Rideout JR, Dillon MR, Bokulich NA, Abnet CC, Al-Ghalith GA, Alexander H, Alm EJ, Arumugam M, Asnicar F, Bai Y, Bisanz JE, Bittinger K, Brejnrod A, Brislawn CJ, Brown CT, Callahan BJ, Caraballo-Rodríguez AM, Chase J, Cope EK, Da Silva R, Diener C, Dorrestein PC, Douglas GM, Durall DM, Duvallet C, Edwardson CF, Ernst M, Estaki M, Fouquier J, Gauglitz JM, Gibbons SM, Gibson DL, Gonzalez A, Gorlick K, Guo J, Hillmann B, Holmes S, Holste H, Huttenhower C, Huttley GA, Janssen S, Jarmusch AK, Jiang L, Kaehler BD, Kang KB, Keefe CR, Keim P, Kelley ST, Knights D, et al. 2019. Reproducible, interactive, scalable and extensible microbiome data science using QIIME 2. *Nat Biotechnol* 37:852–857. <https://doi.org/10.1038/s41587-019-0209-9>.
33. Callahan BJ, McMurdie PJ, Rosen MJ, Han AW, Johnson AJ, Holmes SP. 2016. DADA2: high-resolution sample inference from Illumina amplicon data. *Nat Methods* 13:581–583. <https://doi.org/10.1038/nmeth.3869>.
34. Quast C, Pruesse E, Yilmaz P, Gerken J, Schweer T, Yarza P, Peplies J, Glöckner FO. 2013. The SILVA ribosomal RNA gene database project: improved data processing and web-based tools. *Nucleic Acids Res* 41: D590–D596. <https://doi.org/10.1093/nar/gks1219>.

35. Bokulich NA, Kaehler BD, Rideout JR, Dillon M, Bolyen E, Knight R, Huttley GA, Gregory Caporaso J. 2018. Optimizing taxonomic classification of marker-gene amplicon sequences with QIIME 2's q2-feature-classifier plugin. *Microbiome* 6:90. <https://doi.org/10.1186/s40168-018-0470-z>.
36. Hill TC, Walsh KA, Harris JA, Moffett BF. 2003. Using ecological diversity measures with bacterial communities. *FEMS Microbiol Ecol* 43:1–11. <https://doi.org/10.1111/j.1574-6941.2003.tb01040.x>.
37. Segata N, Izard J, Waldron L, Gevers D, Miropolsky L, Garrett WS, Huttenhower C. 2011. Metagenomic biomarker discovery and explanation. *Genome Biol* 12:R60. <https://doi.org/10.1186/gb-2011-12-6-r60>.
38. Chong J, Liu P, Zhou G, Xia J. 2020. Using MicrobiomeAnalyst for comprehensive statistical, functional, and meta-analysis of microbiome data. *Nat Protoc* 15:799–821. <https://doi.org/10.1038/s41596-019-0264-1>.
39. Dhariwal A, Chong J, Habib S, King IL, Agellon LB, Xia J. 2017. MicrobiomeAnalyst: a web-based tool for comprehensive statistical, visual and meta-analysis of microbiome data. *Nucleic Acids Res* 45:W180. <https://doi.org/10.1093/nar/gkx295>.
40. Douglas GM, Maffei VJ, Zaneveld JR, Yurgel SN, Brown JR, Taylor CM, Huttenhower C, Langille MGI. 2020. PICRUSt2 for prediction of metagenome functions. *Nat Biotechnol* 38:685–688. <https://doi.org/10.1038/s41587-020-0548-6>.
41. Parks DH, Tyson GW, Hugenholtz P, Beiko RG. 2014. STAMP: statistical analysis of taxonomic and functional profiles. *Bioinformatics* 30:3123–3124. <https://doi.org/10.1093/bioinformatics/btu494>.
42. Cai Y, Weng K, Guo Y, Peng J, Zhu Z-J. 2015. An integrated targeted metabolomic platform for high-throughput metabolite profiling and automated data processing. *Metabolomics* 11:1575–1586. <https://doi.org/10.1007/s11306-015-0809-4>.
43. Xia J, Wishart DS. 2010. MetPA: a web-based metabolomics tool for pathway analysis and visualization. *Bioinformatics* 26:2342–2344. <https://doi.org/10.1093/bioinformatics/btq418>.
44. Kim D, Langmead B, Salzberg SL. 2015. HISAT: a fast spliced aligner with low memory requirements. *Nat Methods* 12:357–360. <https://doi.org/10.1038/nmeth.3317>.
45. Liao Y, Smyth GK, Shi W. 2014. featureCounts: an efficient general purpose program for assigning sequence reads to genomic features. *Bioinformatics* 30:923–930. <https://doi.org/10.1093/bioinformatics/btt656>.
46. Liao Y, Smyth GK, Shi W. 2013. The Subread aligner: fast, accurate and scalable read mapping by seed-and-vote. *Nucleic Acids Res* 41:e108. <https://doi.org/10.1093/nar/gkt214>.
47. Love MI, Huber W, Anders S. 2014. Moderated estimation of fold change and dispersion for RNA-seq data with DESeq2. *Genome Biol* 15:550. <https://doi.org/10.1186/s13059-014-0550-8>.
48. Yu G, Wang LG, Han Y, He QY. 2012. clusterProfiler: an R package for comparing biological themes among gene clusters. *OMICS* 16:284–287. <https://doi.org/10.1089/omi.2011.0118>.
49. Bouhaddani SE, Uh H-W, Jongbloed G, Hayward C, Klarić L, Kielbasa SM, Houwing-Duistermaat J. 2018. Integrating omics datasets with the OmicsPLS package. *BMC Bioinformatics* 19:371. <https://doi.org/10.1186/s12859-018-2371-3>.